ACKNOWLEDGMENTS

First, we would like to extend the most profound thanks to Professor C. D. Jeffries for his constant encouragement and support of this work. We also gratefully acknowledge the assistance, at various times in the experiments, of S. Yngvesson, A. Winnacker, and G. Baldacchini. And a few of the many other individuals with whom we have had fruitful discussions are W. B. Fowler, S. Geschwind, J. Margerie, Y. Merle D'Aubigne, D. Schmid, and H. Seidel.

*Research supported in part by the U. S. Atomic Energy Commission, Report No. UCB-34P20-149.

[1]N. V. Karlov, J. Margerie, and Y. Merle-D'Aubigne, J. Phys. (Paris) 24, 717 (1963).

[2]J. Mort, F. Lüty, and F. C. Brown, Phys. Rev. 137, A566 (1965).

[3]H. Panepucci and L. F. Mollenauer, Phys. Rev. 178, 589 (1969).

[4]D. Schmid and V. Zimmerman, Phys. Letters 27A, 459 (1968).

[5]L. F. Mollenauer, S. Pan, and S. Yngvesson, Phys. Rev. Letters 23, 689 (1969).

[6]L. F. Mollenauer, S. Pan, and A. Winnacker, Phys. Rev. Letters 26, 1643 (1971).

[7]W. B. Fowler, in *Physics of Color Centers*, edited by W. B. Fowler (Academic, New York, 1968).

[8]M. P. Fontana and D. B. Fitchen, Phys. Rev. Letters 23, 1497 (1969).

[9]M. P. Fontana, Phys. Rev. B 2, 4304 (1970).

[10]L. F. Mollenauer and G. Baldscchini (unpublished).

[11]F. Porret and F. Lüty, Phys. Rev. Letters 26, 843 (1971).

[12]Y. Ruedin, P. A. Schnegg, M. A. Aegerter, and C. Jaccard, Proceeding of 1971 International Conference on Colour Centres in Ionic Crystals at Reading, England, 1971 (unpublished), see abstracts 48 and 49.

[13]K. H. Becker and H. Pick, Nachr. Akad. Wiss. Göttingen, II Math-Physik K1, 167, (1956).

[14]M. P. Fontana [Phys. Rev. B 2, 4304 (1970)] has made the assumption that $P' = \pm P_s$ for saturated pumping with σ^+ or σ^- light, whereas we have shown here that $P' = 0$ under those conditions. Therefore, his conclusion that spin-dependent polarization effects in the luminescence are immeasurably small is based on a false premise. This has also been shown recently by Baldacchini (see Ref. 10). Thus, Fontana's conclusion about λ in the RES is also groundless.

[15]See any standard text on the resonance phenomenon. Here τ plays the role of T_2.

[16]H. Seidel and H. C. Wolf, in *Physics of Color Centers*, edited by W. B. Fowler (Academic, New York, 1968), p. 555.

[17]H. Mahr, in Ref. 16, p. 270.

[18]Reference 16, Appendix B, p. 627.

[19]Abragam and Bleaney, *Electron Paramagnetic Resonance of Transition Ions* (Clarendon, Oxford, 1970), pp. 221–222.

[20]H. Seidel, Z. Physik 165, 218 (1961).

[21]W. B. Fowler, in Ref. 16.

PHYSICAL REVIEW B VOLUME 6, NUMBER 3 1 AUGUST 1972

Spin Mixing and Magnetic Circular Dichroism in the Absorption Band of *F* Centers–A Theoretical Investigation of Electron-Spin Memory*

A. Winnacker† and L. F. Mollenauer
Department of Physics, University of California, Berkeley, California 94720
(Received 14 February 1972)

A theoretical model of the *F*-center absorption band is described. From it are calculated both the magnetic circular dichroism (MCD) and the spin mixing in the optical-pumping cycle. Despite the fact that it is based on the sometimes doubtful adiabatic approximation, in general, agreement with experiment is good. In particular, it shows that a moderately large MCD effect will be accompanied by a relatively small degree of spin mixing.

I. INTRODUCTION

In this paper two interrelated phenomena, associated with the optical pumping of *F* centers in alkali halides, are investigated from a theoretical point of view: the spin memory, and the magnetic circular dichroism (MCD) of the absorption band. These two phenomena have been discussed in length phenomenologically and experimentally in the foregoing work,[1] henceforth referred to as I. Therefore, we shall recapitulate here only those facts and definitions that are required to make this paper self-contained. For all details of experimental observation and exploitation of these effects, the reader is referred to I.

The MCD of the *F* absorption band in alkali halides is rather large.[2,3] That is, for right- or left-circularly polarized light propagating along the externally applied field H_0 (σ^+ and σ^- transitions), the fraction $f = (\alpha^+ - \alpha^-)/(\alpha^+ + \alpha^-)$, where

α^+ and α^- are the corresponding absorption coefficients, can be on the order of several tens of percent. Now, for optical pumping with (say) σ^+ light, one has rates u^+ and u^- out of the ground-state sublevels $M_s = +\frac{1}{2}$ and $M_s = -\frac{1}{2}$, respectively. It was shown in I that these rates are also related to each other as $(u^+ - u^-)/(u^+ + u^-) = f_p$, where f_p, the paramagnetic contribution to f, is nearly as large as f itself (see I). Thus f also determines the ground-state spin polarization achieved by saturated optical pumping, where by the term "saturated," we mean that the pumping is strong enough to overwhelm spin-lattice relaxation.

However, at a given light intensity and wavelength, the efficiency of the optical pumping depends on yet another property of the system, the spin-mixing parameter ϵ. By definition, ϵ is the fraction of pump cycles for which a transition $\Delta M_s = \pm 1$ occurs. In I, where the rate equations have been solved, it is shown that the spin-pumping time T_p is given by $T_p = [\epsilon(u^+ + u^-)]^{-1}$. This means that a spin mixing $\epsilon > 0$ is required for the optical pumping to affect the spins. Experimentally, ϵ turns out to be a few percent in KCl and KBr; thus the spin memory is not completely but largely conserved in the optical-pumping cycle.[4]

The processes which may lead to spin mixing are as follows: absorption into mixed spin states in the band (ϵ_1); nonradiative decay into the relaxed-excited state (ϵ_2); spin mixing in relaxed-excited state (ϵ_3); and finally, nonradiative decay to the normal ground state (ϵ_4). Since the over-all spin-mixing parameter ϵ is small relative to unity, it should be related to these by the following:

$$\epsilon \cong \epsilon_1 + \epsilon_2 + \epsilon_3 + \epsilon_4. \tag{1}$$

In I it was argued that $\epsilon_3 + \epsilon_4 \ll \epsilon_1 + \epsilon_2$; thus one has $\epsilon \cong \epsilon_1 + \epsilon_2$. Furthermore, the theoretical values for ϵ_1 calculated in this paper are nearly as large as ϵ itself. Thus, except perhaps for the case where ϵ is very small (as in KCl, for example, where $\epsilon = 0.01$),[4] one probably has $\epsilon \sim \epsilon_1$.

Thus the theoretical problem is to produce a model of the F absorption band, for which ϵ_1 is small, while the MCD fraction f is permitted to remain relatively large. We present such a model, based on the idea of Henry, Schnatterly, and Slichter,[5] that phonon-induced deviations of the crystal field from cubic symmetry represent a significant term in the Hamiltonian. That is to say, the noncubic terms are often large relative to the spin-orbit coupling. The principal result of our theory is that, at least approximately, one has $\epsilon_1 = (f_p^0)^2$, where f_p^0 is the maximum absolute value of f_p across the band.

Perhaps it should be explicitly pointed out that the large spin memory is completely at odds with the much-invoked alkali-atom model. In that model, the band is divided into $^2P_{3/2}$ and $^2P_{1/2}$ parts, each rigidly shifted from the other to yield a spin-orbit splitting. The spin projection is highly mixed in such eigenstates of the total angular momentum; for example, one can easily calculate from the Clebsch-Gordon coefficients that $\epsilon_1 = \frac{1}{3}$ for the $P_{1/2}$ part of the band. Thus, there is a strong and direct contradiction between the alkali-atom model and experiment.

Now it has already been shown by Henry and Slichter,[6] that the alkali-atom model is in disagreement with a careful moments analysis of the MCD. Thus the comments of the preceding paragraph may seem unnecessary. However, it is our experience that the alkali-atom model still enjoys a rather widespread, if undeserved, popularity. After all, it does correctly explain the *first-order* band moments $\overline{E}^+$ and $\overline{E}^-$ of the MCD, where the + and − refer to σ^+ and σ^- transitions. $\overline{E}^\pm$ is defined by

$$\overline{E}^\pm = \int_{\text{band}} E\, g^\pm(E)\, dE, \tag{2}$$

where E is the photon energy and where $g^\pm(E)$ are line-shape functions whose integrals over the band equal unity. The difficulty would seem to lie with the remoteness of argument and the experimental uncertainties associated with an analysis of higher-order band moments. On the other hand, arguments based on the large spin memory would seem to have a great advantage of directness and force. Thus, perhaps this work will finally put to rest a model that should have been retired long ago.

The rest of the paper is organized as follows: In Sec. II we write down and discuss the Hamiltonian. Section III is intended to expose the underlying physical ideas, by considering a particular lattice distortion and by calculating the wave functions, spin memory, and MCD in first-order perturbation theory for the case that the distortion term is much bigger than the spin-orbit term. Although the distortion arises from a zero-point phonon, it will be treated as if it were static. In Sec. IV, the calculations are carried through for all possible lattice distortions in accordance with the symmetry of the system, and for all values of strength of the distortion term relative to the spin-orbit interaction. It will turn out that for all possible distortions, with the exception of the so-called "breathing mode," ϵ_1 is small whenever the distortion term is large relative to the spin-orbit term. Here still the distortions are treated as if they were static. In Sec. V, finally, the dynamic character of the distortion is accounted for, by taking appropriate averages over the normal coordinates of the lattice vibrations in the frame of the configuration-coordinate model; that is, the averages are taken over adiabatic wave functions and transition probabilities. The treatment is thus similar to the one given by Moran[7] to calculate the

line shape of the F absorption in the cesium halides; in particular, the most basic assumptions are the same. Their validity for our calculations will be discussed in that chapter. However, the adiabatic wave functions must be calculated exactly in our case, by diagonalizing the perturbation Hamiltonian. This exact treatment is necessary because, for potassium halides, the spin-orbit interaction is generally not large compared to the phonon interaction, as is assumed for the cesium halides.

II. HAMILTONIAN

In the following we will use notation and a format similar to that of Henry and Slichter, such that the reader may more easily compare the somewhat specialized treatment of this work with their more general one.[6] Let the F electron have spin $\vec{S}$ and position $\vec{r}$, and let the surrounding lattice be described by normal coordinates Q_i. Then the Hamiltonian which describes the resultant coupled system is given by the expression:

$$\mathcal{H}=\mathcal{H}_E(\vec{r})+\mathcal{H}_L(Q)+\mathcal{H}_{el}(r,Q)+\mathcal{H}_{so}(\vec{r},\vec{S})+\mathcal{H}_Z(\vec{r},\vec{S}), \tag{3}$$

where Q should be understood to represent the complete ensemble of Q_i. $\mathcal{H}_E$ refers to the electron without spin-orbit coupling, and with the lattice fixed in the equilibrium positions, $Q_i=0$. $\mathcal{H}_L(Q)$ is just a sum of simple-harmonic-oscillator Hamiltonians, one for each of the Q_i. $\mathcal{H}_{el}(\vec{r},\vec{Q})$ describes the change, due to lattice distortions, in the electron-lattice potential; hence it is zero whenever all of the $Q_i=0$. $\mathcal{H}_{so}=\lambda\,\vec{L}\cdot\vec{S}$ is the spin-orbit interaction where L and S are in units of $\hbar$, such that the spin-orbit parameter λ will have units of energy. Approximate values of λ have been deduced from MCD measurements, and they are typically of order $\lambda\sim 10$–50 meV. $\mathcal{H}_Z$ is the Zeeman term, $\mathcal{H}_Z=\mu_B H_0(L_Z+2S_Z)$, where μ_B is the Bohr magneton, H_0 is the externally applied field, and again L and S are in units of $\hbar$. Throughout this paper we assume $\mathcal{H}_Z$ to be much smaller than either $\mathcal{H}_{el}$ or $\mathcal{H}_{so}$. That is, $\mathcal{H}_Z$ is supposed to lift magnetic degeneracies, while wave function admixing due to $\mathcal{H}_Z$ is ignored in deference to the much larger effects of $\mathcal{H}_{so}$.

Phonons of the alkali-halide lattice may be classified according to their symmetry properties. The desired symmetries are those of basis functions of the irreducible representations of the cubic-point-symmetry group O_h. In Ref. 6, it is shown that only those phonon modes belonging to one of six symmetry types will lead to nonzero matrix elements of $\mathcal{H}_{el}$ for p states. The irreducible representations and typical basis functions corresponding to the required six symmetries are tabulated:

$$\Gamma_1^+ \text{ or } A_{1g}\text{: } x^2+y^2+z^2=f_1(\vec{r});$$

$$\Gamma_3^+ \text{ or } E_g\text{: } \begin{cases} 2z^2-x^2-y^2=f_2(\vec{r}), \\ \sqrt{3}\,(x^2-y^2)=f_3(\vec{r}); \end{cases}$$

$$\Gamma_5^+ \text{ or } T_{2g}\text{: } \begin{cases} yz=f_4(\vec{r}), \\ zx=f_5(\vec{r}), \\ xy=f_6(\vec{r}). \end{cases} \tag{4}$$

By assuming that the leading terms in the ion potential arising from a displacement are linear in the normal coordinates Q_i, one may write[6]

$$\mathcal{H}_{el}=\sum_{i=1}^{6} V_i(\vec{r})\,Q_i, \tag{5}$$

where each V_i in (5) above has the same symmetry as the corresponding f_i in (4).

III. EFFECTS OF STRONG QUASISTATIC DISTORTION

In order to illustrate the basic idea of this paper, let us first consider the effects of a single mode. That is, in Eq. (5), let all the Q_i be zero but one. For example, let us choose Q_3, associated with the function f_3 of (4). There is no z motion in this mode, and when the surrounding ions move in along the x axis, they move out an equal amount along the y axis. The matrix representation of $\mathcal{H}_{el}(\vec{r},Q_3)$ will be diagonal in the p-state basis set $|x+\rangle$, $|x-\rangle$, $|y+\rangle$, $|y-\rangle$, $|z+\rangle$, $|z-\rangle$, where the + and − refer to $m_S=\pm\frac{1}{2}$. $\mathcal{H}_{el}(\vec{r},Q_3)$ raises the $|x\pm\rangle$ state energies by an amount $\frac{1}{2}D$ (this defines D for the Q_3 mode); it does not affect $|z\pm\rangle$, and it lowers $|y\pm\rangle$ by $\frac{1}{2}D$.

By calculating the matrix elements of $\mathcal{H}_{so}$ with respect to the above basis, we then obtain the following representation of $\mathcal{H}_{el}+\mathcal{H}_{so}$:

	$\lvert x+\rangle$	$\lvert x-\rangle$	$\lvert y+\rangle$	$\lvert y-\rangle$	$\lvert z+\rangle$	$\lvert z-\rangle$
$\lvert x+\rangle$	$\frac{1}{2}D$	0	$-i\frac{1}{2}\lambda$	0	0	$\frac{1}{2}\lambda$
$\lvert x-\rangle$	0	$\frac{1}{2}D$	0	$i\frac{1}{2}\lambda$	$-\frac{1}{2}\lambda$	0
$\lvert y+\rangle$	$i\frac{1}{2}\lambda$	0	$-\frac{1}{2}D$	0	0	$-i\frac{1}{2}\lambda$
$\lvert y-\rangle$	0	$-i\frac{1}{2}\lambda$	0	$-\frac{1}{2}D$	$-i\frac{1}{2}\lambda$	0
$\lvert z+\rangle$	0	$-\frac{1}{2}\lambda$	0	$i\frac{1}{2}\lambda$	0	0
$\lvert z-\rangle$	$\frac{1}{2}\lambda$	0	$i\frac{1}{2}\lambda$	0	0	0

(6)

By treating as a perturbation that part of the matrix (6), which represents $\mathcal{H}_{so}$, we obtain the following wave functions to first order in the parameter λ/D:

$$\begin{aligned}
\psi_x^+ &= |x+\rangle + \frac{i}{2}\frac{\lambda}{D}|y+\rangle + \frac{\lambda}{D}|z-\rangle,\\
\psi_x^- &= |x-\rangle - \frac{i}{2}\frac{\lambda}{D}|y-\rangle - \frac{\lambda}{D}|z+\rangle,\\
\psi_y^+ &= |y+\rangle + \frac{i}{2}\frac{\lambda}{D}|x+\rangle - i\frac{\lambda}{D}|z-\rangle,\\
\psi_y^- &= |y-\rangle - \frac{i}{2}\frac{\lambda}{D}|x-\rangle - i\frac{\lambda}{D}|z+\rangle,\\
\psi_z^+ &= |z+\rangle + \frac{\lambda}{D}|x-\rangle - i\frac{\lambda}{D}|y-\rangle,\\
\psi_z^- &= |z-\rangle - \frac{\lambda}{D}|x+\rangle - i\frac{\lambda}{D}|y+\rangle.
\end{aligned} \tag{7}$$

For convenience in calculating σ^+ and σ^- transition probabilities, the wave functions should be rewritten in terms of the states $|x \pm iy\rangle$, as, for example,

$$\Psi_x^- = \left(\frac{1+\delta}{\sqrt{2}}\right)|x+iy,-\rangle + \left(\frac{1-\delta}{\sqrt{2}}\right)|x-iy,-\rangle - 2\delta|z+\rangle, \tag{8}$$

where $\delta = -\lambda/2D$. For transitions out of the $m_s = -\frac{1}{2}$ ground state only (corresponding to absorption at zero temperature), by using the selection rule $\Delta M_s = 0$, we obtain

$$\begin{aligned}
\Delta E &= \bar{E}^+ - \bar{E}^- = 2\left[\frac{D}{2}\left(\frac{1+\delta}{\sqrt{2}}\right)^2 - \frac{D}{2}\left(\frac{1-\delta}{\sqrt{2}}\right)^2\right]\\
&= 2\delta D = -\lambda\,.
\end{aligned} \tag{9}$$

Taking D as a crude measure of the absorption bandwidth, we then obtain $f_p \sim \lambda/D$, whereas the fractional spin mixing in any part of the band is $\epsilon_1 = (\lambda/D)^2 \sim (f_p^0)^2$.

It will be shown explicitly in the next section that in the limit $\lambda/D \ll 1$, one obtains essentially the same result for each of the Γ_3^+ and Γ_5^+ modes; that is, one always obtains $\epsilon_1 \sim (f_p^0)^2$. On the other hand, a pure "breathing" mode (Γ_1^+ or Q_1) does not destroy cubic symmetry, and hence the orbital momentum of p states is completely preserved. Thus for a pure-Q_1 mode, one obtains the same large degree of spin mixing as for the alkali-atom model. However, the probability that the F center will be subject to a pure-Q_1 mode should be very small. Therefore, it is not unreasonable to maintain $(f_p^0)^2$ as a rough estimate of ϵ_1.

In Table I, we compare the ϵ_1 estimated as $(f_p^0)^2$ with the experimental values of ϵ listed in I. In view of the crude approximations that are involved, the close agreement between ϵ_1 and ϵ_{expt} is probably somewhat fortuitous. But it is quite significant that that ϵ_{expt} scales with $(f_p^0)^2$ in just the manner predicted by the simple perturbation calculation. We are thus led to believe that the basic idea is indeed a correct one.

IV. EFFECTS OF Γ_3^+ AND Γ_5^+ DEFORMATIONS: DETAILED STUDY

In a more realistic treatment, one must calculate the effects of a given mode on the spin mixing for all possible values of D/λ in the range, $|D\lambda| = 0$ to $|D\lambda| \gg 1$, and not just in the limit $|D\lambda| \gg 1$. To make such a calculation, we proceeded as follows; For each of the Γ_3^+ and Γ_5^+ modes, the perturbation matrix $\mathcal{H}_{e1}(Q_i)$ was calculated for the p-state basis set $|x\pm\rangle$, $|y\pm\rangle$, $|z\pm\rangle$ used in Sec. III. The matrix sum $\mathcal{H}_{e1}(Q_i) + \mathcal{H}_{so}$ was then diagonalized exactly by a CDC 6400 computer, for many values of the paramenter D/λ. For each value of D/λ, the computer printout listed three distinct energy eigenvalues, and the components of six distinct eigenvectors. The eigenvectors were degenerate in pairs, and they were such that the degeneracy could be lifted by a magnetic field, without the production of any state mixing in zeroth order. That is, $\mathcal{H}_Z$ was already diagonal in the resultant eigenvectors.

Now let us designate the eigenstates with the notation $\psi_i^\pm$ where the subscript ($i = 1, 2, 3$) indicates the associated energy level, and where + (or −) indicates that member of the degenerate pair that has nearly pure $m_s = +\frac{1}{2}$ (or $m_s = -\frac{1}{2}$) spin character in the limit $D/\lambda \gg 1$. By writing the wave functions $\psi_i^\pm$ in the form

$$\psi_i^\pm = a_i^\pm|m_s = +\tfrac{1}{2}\rangle + b_i^\pm|m_s = -\tfrac{1}{2}\rangle, \tag{10}$$

the fractions of $m_s = +\frac{1}{2}$ and $m_s = -\frac{1}{2}$ states in the wave function can then be written down directly. ψ_i^+ and ψ_i^- are complementary to each other in the sense that $|a_i^+|^2 = |b_i^-|^2$. Hence it is meaningful to speak of the degree of spin mixing ϵ_i associated with each pair of states $\psi_i^\pm$. We define ϵ_i by setting $\epsilon_i = |a_i^-|^2 = |b_i^+|^2$. Thus ϵ_i represents the degree of $m_s = -\frac{1}{2}$ state admixed into ψ_i^+, or equivalently, it represents the degree of $m_s = +\frac{1}{2}$ state admixed into ψ_i^-.

In Figs. 1(a)–1(c), ϵ_i is plotted as a function of D/λ, for the two modes of Γ_3^+ and for one of the Γ_5^+ modes, the zx mode. Since the results for the other two Γ_5^+ modes are essentially the same as for the zx mode, those results have not been shown separately. Note that in all cases, $\epsilon_i \leq \frac{1}{2}(D/\lambda)^{-2}$, for $D/\lambda \gg 1$.

A curve labeled f_p^0 is also given in Figs. 1(a)–1(c), where f_p^0 is the MCD fraction referred to in the Introduction. Let $\Delta E = \bar{E}_0^+ - \bar{E}_0^-$, where $\bar{E}_0^+$ and E_0^- are the first-order band moments for absorption of σ^+ and σ^- light, respectively, at zero temperature and finite field H_0. [$\bar{E}^+$ and $\bar{E}^-$ are defined in Eq. (2)]. Once again, as in Sec. III, we calculate f_p^0 as the ratio of $|\Delta E|$ to the width of the absorption band. Now, our calculations con-

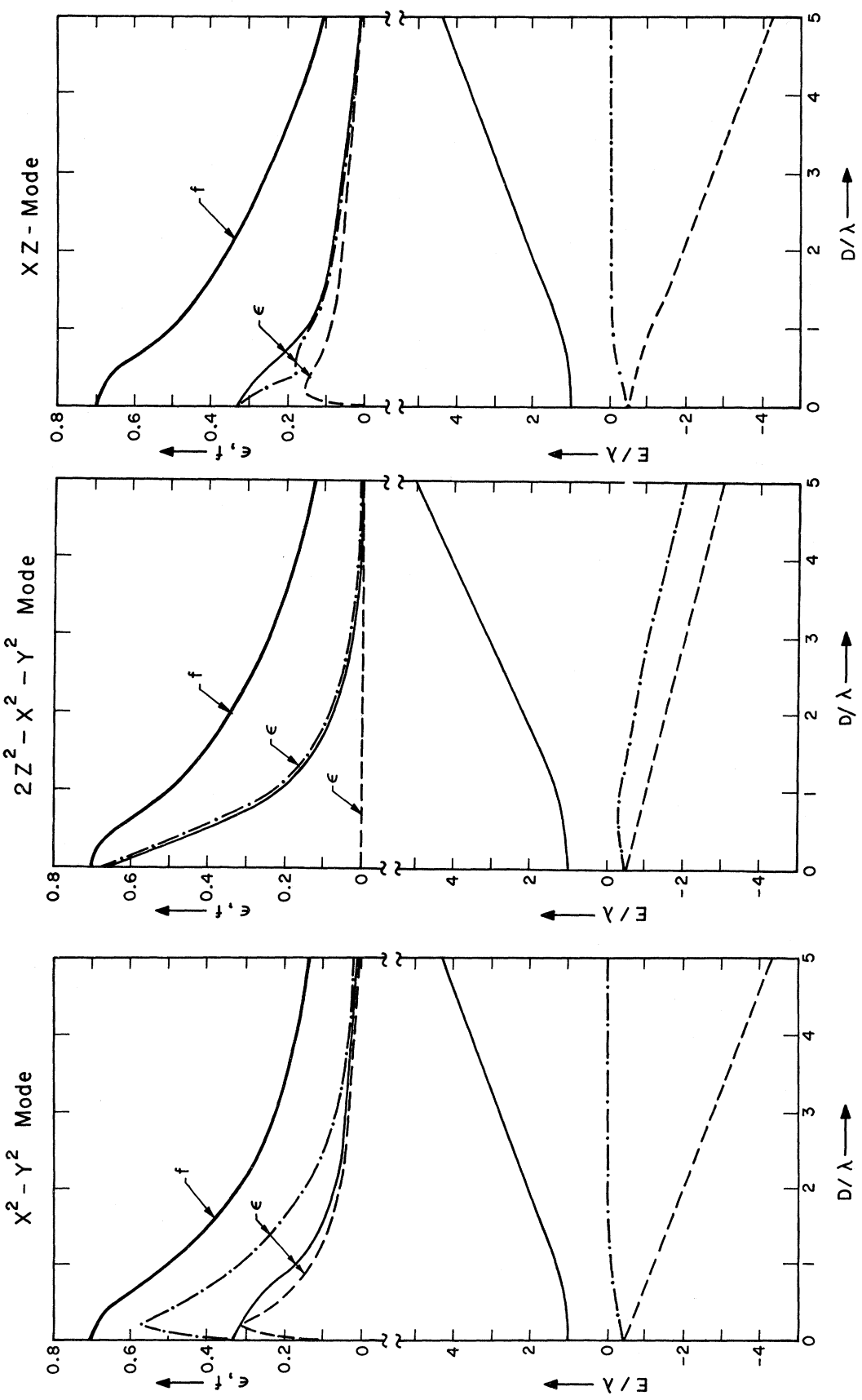

FIG. 1. (a) Effects of a static distortion of x^2-y^2 symmetry on the three p states of the F band that go over to pure $m_s=+\frac{1}{2}$ character at $D/\lambda=\infty$. Above: ϵ for each of the three states as a function of D/λ; f is also shown. Below: Energies of each of the three states as a function of D/λ. D is an effective crystal-field parameter, and λ is the spin-orbit coupling parameter (see text). (b) The quantities of Fig. 1(a) for a distortion of $2z^2-x^2-y^2$ symmetry. (c) The quantities of Fig. 1(c) for a distortion of xz symmetry.

firm the prediction of a more general theorem,[8] that $\Delta E = -\lambda$, independently of the phonon mode acting on the F center, or of the magnitude of D/λ. As a measure of the bandwidth, we use twice the square root of the second moment. With D defined for each mode as indicated by the inserts in Figs. 1(a)–1(c), the bandwidth is always given by the expression $[2(D^2+\lambda^2)]^{1/2}$. Thus, the MCD curve is just a plot of the quantity $f_p^0 = \{2[(D/\lambda)^2+1]\}^{-1/2}$. Note that for $D/\lambda \gg 1$, we have essentially $f_p^0 \cong \sqrt{\frac{1}{2}} \times (\lambda/D)$.

There are a number of important conclusions to be drawn from the above. First, we can confirm the statement made near the end of Sec. III, that for $D/\lambda \gg 1$, one always has $\epsilon_i \cong (f_p^0)^2$. Second, an inspection of Figs. 1(a)–1(c) reveals that the average spin mixing, and the fraction f_p^0, are both nearly the same for all modes, except perhaps in the immediate neighborhood of $D/\lambda = 0$. Thus, it is not unreasonable to suppose that a linear superposition of these modes will produce essentially the same result as any one of them alone. Only the Γ_1 mode fails to reduce the spin mixing. But since the Γ_1 represents only one out of six possible modes, the probability that the system will see a Γ_1 mode, sufficiently pure to enable the system to retain an alkali-atom-like character, should be very small indeed.

V. DYNAMIC TREATMENT

In this section we attempt to account for the dynamic nature of the lattice distortions, in the following manner: The effect of a superposition of lattice distortions is calculated. Again, the distortions are described by the normal coordinates Q_i introduced in Sec. II. The calculation is repeated for many combinations of the various Q_i, and an appropriate average is taken of the results. By appropriate average, we mean that each of the displacements Q_i is weighted according to the probability distribution of a simple-harmonic oscillator in its ground state.

As we have already indicated in the Introduction, the calculation is in many respects similar to one made by Moran[7] on the structure of the F band in the cesium halides. Both are based on the adiabatic approximation. But not all of the approximations that may be used for the cesium halides are suitable for the potassium halides as well. And, of course, we are primarily concerned here with the calculation of the spin memory, a question that Moran did not consider. The differences and similarities of the two calculations are discussed in greater detail below.

A. Underlying Approximations

(i) The validity of the adiabatic approximation has been discussed in Ref. 5 for the case of F centers. By introducing typical quantitative values for the parameters of their model, the authors derive as a very rough criterion for adiabatic motion that the quantity $(\lambda/0.01\ \text{eV})^{3/2}$ be large compared to unity. This condition is fairly well fulfilled for the cesium halides and for KI. (λ of KI is 22.8 meV, λ for CsBr is 28 meV.)[9] But for KBr and KCl, where $\lambda = 12.8$ and 7.6 meV, respectively,[3] the criterion is not satisfied. Hence, the model is probably not too reliable for these latter crystals. On the other hand, the results of Sec. III indicate that calculations based on the adiabatic approximation give the right order of magnitude for ϵ, despite the fact that the use of the adiabatic condition is not truly justified. Therefore, in this section, we will apply the calculations to KBr, although we will focus mainly on the more justifiable case of KI.

(ii) In Moran's calculation, only the breathing mode and the two distortions of Γ_3 symmetry were taken into account. That is, Moran used the following electron-phonon interaction Hamiltonian:

$$\mathcal{H}_{e1} = C_1(x^2+y^2+z^2)S + C_3(2z^2-x^2-y^2)Z + C_3\sqrt{3}\,(x^2-y^2)T, \quad (11a)$$

where S, Z, T are the normal coordinates (Q_i) of the vibrations. It is useful to express (11a) in terms of angular momentum operators:

$$\mathcal{H}_{e1} = -\gamma_1(\tfrac{1}{2}\vec{L}\cdot\vec{L})S - \gamma_3(3L_z^2 - \vec{L}\cdot\vec{L})Z - \gamma_3\sqrt{3}\,(L_x^2 - L_y^2)T. \quad (11b)$$

Using the p-state basis set $|J, M_J\rangle$, where the states $|J, M_J\rangle$ are eigenfunctions of the total angular momentum operators, one obtains the following matrix representation of the operator $\mathcal{H}_{so} + \mathcal{H}_{e1}$:

$$\langle J, M_J | \mathcal{H}_{so} + \mathcal{H}_{e1} | J', M_J' \rangle =$$

	$\left\|\frac{3}{2},\frac{3}{2}\right\rangle$	$\left\|\frac{3}{2},-\frac{1}{2}\right\rangle$	$\left\|\frac{1}{2},-\frac{1}{2}\right\rangle$	$\left\|\frac{3}{2},-\frac{3}{2}\right\rangle$	$\left\|\frac{3}{2},\frac{1}{2}\right\rangle$	$\left\|\frac{1}{2},\frac{1}{2}\right\rangle$
$\left\|\frac{3}{2},\frac{3}{2}\right\rangle$	$\frac{1}{2}\lambda+z+s$	t	$-t/\sqrt{2}$	0	0	0
$\left\|\frac{3}{2},-\frac{1}{2}\right\rangle$	t	$\frac{1}{2}\lambda-z+s$	$-z/\sqrt{2}$	0	0	0
$\left\|\frac{1}{2},-\frac{1}{2}\right\rangle$	$-t/\sqrt{2}$	$-z/\sqrt{2}$	$-\lambda+s$	0	0	0
$\left\|\frac{3}{2},-\frac{3}{2}\right\rangle$	0	0	0	$\frac{1}{2}\lambda+z+s$	t	$-t/\sqrt{2}$
$\left\|\frac{3}{2},\frac{1}{2}\right\rangle$	0	0	0	t	$\frac{1}{2}\lambda-z+s$	$-z/\sqrt{2}$
$\left\|\frac{1}{2},\frac{1}{2}\right\rangle$	0	0	0	$-t/\sqrt{2}$	$-z/\sqrt{2}$	$-\lambda+s$

, (12)

TABLE I. Value of ϵ calculated according to Sec. II, compared with experiment.

Crystal	ϵ_{expt}	$\epsilon_1=(f_p^0)^2$
KCl	0.01	0.0025
KBr	0.04	0.022
KI	0.24	0.16

where $s=-\gamma_1 S$, $t=-\gamma_3 T$, $z=-\gamma_3 Z$.

For our calculations as well, it would be very convenient to include only the Γ_1 and Γ_3 modes. The reason is that in the course of the calculations the above interaction matrix (12) must be diagonalized for a large number of points (s,t,z). As seen from Eq. (12), only one 3×3 matrix must be diagonalized, if only those two types of mode are present. However, taking into account the Γ_5 distortions introduces two additional complications: First, the matrix (12) no longer splits into two identical 3×3 matrices, and second, we obtain complex matrix elements. This leads to an increase, by a factor of at least 8, in the already considerable computation time.

It can be shown[7,8] that the effect of the Γ_5 distortions on the band shape can be included in good approximation by introducing an effective mean-squared interaction

$$\langle E_3^2\rangle_{eff}=\langle E_3^2\rangle+\langle E_5^2\rangle \tag{13}$$

instead of using the mean-squared interactions $\langle E_3^2\rangle$ and $\langle E_5^2\rangle$ of the Γ_3 and Γ_5 distortions as distinct parameters of the theory. The physical reason for the validity of this approach is that the degeneracies of the p states are already lifted by Γ_3 distortions. In fact, this simplication leads only to minor changes in the fourth and higher moments of the band. The same argument holds for our calculation of the MCD effect, since the MCD is, of course, just the difference between two absorption curves.

It is not at first obvious that the above approximation will be valid for the calculation of spin memory as well. On the other hand, Figs. 1(a)–1(c) show that all the various noncubic modes result in a very similar behavior of ϵ as a function of D/λ for $D/\lambda>1$. Thus the calculations of Sec. IV strongly suggest that it does not make much difference whether all the noncubic modes are included, or whether only Γ_3 modes are considered, as long as one introduces the effective interaction of Eq. (13). To check this assumption, in a few typical cases, ϵ was calculated both by including the Γ_5 modes explicitly, and by just using $\langle E_3^2\rangle_{eff}$. No significant difference in the results for ϵ was obtained. Thus the approximation was used for the bulk of the calculations, and we shall discuss the theory within that framework.

(iii) In his treatment of the cesium halides, Moran was able to use first-order perturbation theory. That is, it is not a bad approximation for the cesium halides to assume that $\langle\mathcal{H}_{so}\rangle\gg\langle\mathcal{H}_{el}\rangle$. However, that approximation is not at all valid for the potassium halides, where the linewidth is due largely to phonons. In the potassium halides, the quantities s,t,z of matrix (12) assume values larger as well as smaller than λ. Thus, as we have already asserted in the Introduction, the adiabatic wave functions must be calculated by exact diagonalization of the matrix (12).

B. Calculations

For a given set of normal coordinates s,t,z, the adiabatic wave functions of the absorption state are calculated by diagonalizing the Hamiltonian. As the Hamiltonian consists of two 3×3 submatrices, we obtain two sets of wave functions ψ and ϕ, which are superpositions of $|\frac{3}{2},\frac{3}{2}\rangle$, $|\frac{3}{2},-\frac{1}{2}\rangle$, $|\frac{1}{2},-\frac{1}{2}\rangle$ and $|\frac{3}{2},-\frac{3}{2}\rangle$, $|\frac{3}{2},\frac{1}{2}\rangle$, $|\frac{1}{2},\frac{1}{2}\rangle$, respectively:

$$\psi_i=a_1^i(s,t,z)\left|\tfrac{3}{2},\tfrac{3}{2}\right\rangle+a_2^i(s,t,z)\left|\tfrac{3}{2},-\tfrac{1}{2}\right\rangle+a_3^i(s,t,z)\left|\tfrac{1}{2},-\tfrac{1}{2}\right\rangle, \tag{14}$$

with eigenvalues E_i, $i=1,2,3$, and

$$\phi_i=b_1^i(s,t,z)\left|\tfrac{3}{2},-\tfrac{3}{2}\right\rangle+b_2^i(s,t,z)\left|\tfrac{3}{2},\tfrac{1}{2}\right\rangle+b_3^i(s,t,z)\left|\tfrac{1}{2},\tfrac{1}{2}\right\rangle, \tag{15}$$

with eigenvalues E_i', $i=1,2,3$. Because the two submatrices are identical, ψ_i and ϕ_i are the Kramers degenerate; i.e., the following relations hold:

$$a_j^i=b_j^i, \tag{16a}$$

$$E_i=E_i' \tag{16b}$$

for all i and j. However, for the purpose of further discussion, we consider the degeneracy (16b) to be lifted by a small magnetic field in the sense described in the context of Eq. (3). Hence, we now have $E_i\neq E_i'$, but also $E_i\cong E_i'$.

To calculate the transition probabilities for $\sigma^{\pm}$ transitions, which are governed by the selection rules $\Delta m_l=\pm1$, it is convenient to switch from the above $|J,M_J\rangle$ representation to the $|m_l,m_s\rangle$ representation, as, for example,

$$\left|\tfrac{3}{2},\tfrac{3}{2}\right\rangle=\left|1,\tfrac{1}{2}\right\rangle,$$
$$\left|\tfrac{3}{2},-\tfrac{1}{2}\right\rangle=\sqrt{\tfrac{2}{3}}\left|0,-\tfrac{1}{2}\right\rangle+\sqrt{\tfrac{1}{3}}\left|-1,+\tfrac{1}{2}\right\rangle, \text{ etc.} \tag{17}$$

By substituting expansions of the form (17) into (14) and (15), it is easy to compute the following *relative* transition probabilities. For σ^+ absorption out of the $m_s=+\frac{1}{2}$ ground-state sublevel, one has

$$u_i^+=|a_1^i|^2 \quad \text{into } \psi_i,$$
$$u_i^+=0 \quad \text{into all } \phi_i. \tag{18}$$

For σ^+ absorption out of the $m_s=-\frac{1}{2}$ ground-state sublevel, one has

$$u_i^- = 0 \quad \text{into all } \psi_i,$$
$$u_i^- = \tfrac{1}{3}\left|b_2^i\right|^2+\tfrac{2}{3}\left|b_3^i\right|^2+\tfrac{2}{3}\sqrt{2}\left|b_2^i b_3^i\right| \quad \text{into } \phi_i. \quad (19)$$

[By time-reversal symmetry, σ^- absorption probabilities out of $m_s=-\frac{1}{2}$ will be given by (18), and σ^- probability out of $m_s=+\frac{1}{2}$ will be given by (19), if the roles of ψ and ϕ are interchanged everywhere.] Thus, we can calculate the MCD fraction

$$f=(u^+-u^-)/u^++u^-) \quad (20)$$

for any adiabatic wave function. [In I, the symbol u was used to designate an actual transition *rate*. However, since we deal here only with ratios of rates, as in (20), we need consider only the dimensionless quantities given by Eqs. (18) and (19).]

We define the spin-mixing parameter ϵ_i for the ψ_i states to be the probability that the spin has projection $m_s=-\frac{1}{2}$ in these states. This is a reasonable definition, since two of the three ψ_i states go over to pure $m_s=+\frac{1}{2}$ character, whenever t or z becomes very large relative to λ. In the same limit, the third of the states ψ_i becomes the state $|0,-\frac{1}{2}\rangle$ in the $|m_l,m_s\rangle$ representation; but since this latter state never participates in a $\sigma^\pm$ absorption from the ground state, its $m_s=-\frac{1}{2}$ character does not affect the value of expression (26) for the average value of ϵ. For the Kramers-conjugate states ϕ_i, we define $\epsilon_i'=\epsilon_i$. Thus, by writing Eq. (14) or (15) explicitly in terms of the $|m_l,m_s\rangle$ representation, one calculates immediately that

$$\epsilon_i=\left|\sqrt{\tfrac{2}{3}}\,a_2^i+\sqrt{\tfrac{1}{3}}\,a_3^i\right|^2=\left|\sqrt{\tfrac{2}{3}}\,b_2^i+\sqrt{\tfrac{1}{3}}\,b_3^i\right|^2. \quad (21)$$

It will undoubtedly be noted that the above definition of ϵ_i is not identical to that given in Sec. IV of this paper. However, in the calculation of an average ϵ, as by Eq. (26), the two approaches should yield the same final result.

Now that we have expressions for the MCD effect and for the spin mixing, in terms of the parameters s,t,z, and λ, it is time to calculate the "appropriate averages" mentioned earlier. As normal coordinates of simple-harmonic vibrations, s,t,z show Gaussian probability distributions in the ground state. Using the notation of Ref. 7, we write

$$P_1(s)\,ds=\frac{1}{(2\pi W_1^2)^{1/2}}\,e^{-s^2/2W_1^2}\,ds,$$
$$P_3(t)\,dt=\frac{1}{(\pi W_3^2)^{1/2}}\,e^{-t^2/W_3^2}\,dt, \quad (22)$$
$$P_3(z)\,dz=\frac{1}{(\pi W_3^2)^{1/2}}\,e^{-z^2/W_3^2}\,dz,$$

where the quantities P are probability densities, and where W_1 and W_3 are the rms interactions with the symmetric mode and with either of the Γ_3 modes, respectively. That is, the three distortions make a contribution $W_1^2+2W_3^2$ to the second moment of the line.

Calculation of the MCD fraction for light of energy E begins with evaluation of the following quantities:

$$U^\pm(E)=\sum_i\int U_i^\pm(s,t,z)\,P_1(s)P_3(t)P_3(z)\times\delta\left(E_i(s,t,z)-E\right)ds\,dt\,dz. \quad (23)$$

The MCD fraction $f(E)$ is then just given by

$$f(E)=\frac{U^+(E)-U^-(E)}{U^+(E)+U^-(E)}. \quad (24)$$

For easy comparison with experiment, it is often convenient to work with the following quantity:

$$f'(E)=\frac{U^+(E)-U^-(E)}{U^+(E_0)+U^-(E_0)}, \quad (25)$$

where E_0 is some fixed photon energy in the band, usually at the band center.

The spin-mixing parameter ϵ is computed from the following expression:

$$\epsilon(E)=\left[\sum_i\int U_i^+(s,t,z)P_1(s)P_3(t)P_3(z)\,\epsilon_i(s,t,z)\times\delta(E_i(s,t,z)-E)\,ds\,dt\,dz\right](U^+)^{-1}. \quad (26)$$

Equation (26) was derived by consideration of a σ^+ absorption out of the $m_s=\frac{1}{2}$ state. (By time-reversal symmetry, an identical expression results from consideration of a σ^- absorption from the $m_s=-\frac{1}{2}$ state.) Thus, the $\epsilon_i\,(s,t,z)$ will be weighted according to the probability that the corresponding $\psi_i(s,t,z)$ will be the actual terminal state of the transition.

Consideration of a σ^+ absorption out of the $m_s=-\frac{1}{2}$ state (or of σ^- out of $m_s=\frac{1}{2}$) will yield an expression for ϵ the same as (26) if u_i^+ and U^+ are replaced with u_i^- and U^-, respectively. It is not clear that the two expressions will have the same value in all cases, but at least they ought to become equal in the limit that ϵ is very small. Unfortunately, only the ϵ given by (26) was evaluated in the computer calculations.

In the actual calculations of expressions (23) and (26), the F band is divided into small energy intervals of width Δ, and the δ functions are then replaced by the functions

$$F_i(s,t,z)=\begin{cases}1 & \text{if } E-\frac{1}{2}\Delta<E_i<E+\frac{1}{2}\Delta\\ 0 & \text{otherwise.}\end{cases} \quad (27)$$

This means that the quantities $U^\pm(E)$ and $\epsilon(E)$ were calculated for photons within the energy interval Δ around E. The multiple integrals were calculated by Monte Carlo integration. Thus, the computer program proceeded as follows: First, random points s,t,z were created by the computer within the integration area:

TABLE II. Values of ϵ and f' for potassium halides, calculated according to Sec. V, and compared with experiment.

Crystal	f'_{expt}	f'_{calc}	ϵ_{expt}	ϵ_{calc}
KBr	0.15	0.188	0.04	0.107
KI	0.4	0.31	0.24	0.202

$$-3W_1 \leq s \leq +3W_1, \quad -3W_3 \leq z, t \leq +3W_3 . \tag{28}$$

Contributions from outside these domains can be neglected, because P_1 and P_3 are small there. For the random points s, t, z, the matrix (12) was diagonalized and the wave functions ψ_i and ϕ_i were calculated. From the wave functions then are obtained the quantities $u_i^*(s,t,z)$ and $\epsilon_i(s,t,z)$, according to Eqs. (18), (19), and (21). The program then determines the energy interval of width Δ to which the eigenvalue of the wave function belongs, i.e., it determines the value of $F_i(s,t,z)$. Finally, the Monte Carlo integration is carried out by averaging over the values of the integrands and multiplying by the area of integration.

Finally, it should be mentioned that the Γ_5 modes can be included very easily in this program. If the normal coordinate of such a mode is called v, we have only to take the Gaussian probability distribution $P(v)$ as an additional factor into the integrand, include the matrix elements of the mode into the interaction Hamiltonian (12), and let the computer choose random values s, t, z, v in the now four-dimensional integration space to perform the Monte Carlo integration. However, as discussed earlier, this was done only for a few selected values of the parameters, on account of the large increase in calculation time caused by the higher order of the matrix.

C. Results

The mathematical model given above has been used to calculate the spin memory, the MCD fraction f', and the total absorption. All three quantities were calculated as a function of the incident photon energy, and for appropriate values of the parameters W_1, W_3, and λ. Thus, the theory may be compared in a very complete and meaningful way with the experimentally known MCD and absorption band shapes. Although $\epsilon(E)$ is known experimentally for only a narrow range of energies, comparison with the theoretical curve is still quite meaningful, since the curve is essentially flat over the middle of the absorption band. In general, agreement between theory and experiment is quite good. Selection of input parameters, and comparison of theory with experiment are discussed in detail below.

The parameters W_1 and W_3 have been determined by Schnatterly in a moment analysis of stress experiments on the F band.[6] From Ref. 6 and the relations:

$$W_1^2 = \langle E_1^2 \rangle, \quad W_3^2 = \tfrac{1}{2}(\langle E_3^2 \rangle + \langle E_5^2 \rangle), \tag{29}$$

we obtain the ratios $W_1/W_3 = 1.63$, 3.0, and 2.15 for KCl, KBr, and KI, respectively. To show the dependence of f' and ϵ on the relative strength of phonon interaction and spin-orbit coupling, we varied W_3/λ for a fixed "typical" ratio W_1/W_3; that is, we set $W_1/W_3 = 2.15$, the value appropriate to KI. The results are shown in Fig. 2, where f' and ϵ have been calculated for a photon energy corresponding to one of the peaks in the f' curve. Qualitatively, f' and ϵ show a behavior similar to that expressed in Fig. 1. However, the decrease with increasing W_3/λ is less pronounced. This is to be expected, since the vibrations, treated as quantum-mechanical oscillators in their ground state, show a maximum in their probability distribution for small distortions.

But λ is also known, as discussed previously. Thus, in fact, there are no adjustable parameters. For KI, we have $\lambda = 22.8$ meV[8] and $W_3 = 27$ meV,[6] corresponding to $W_3/\lambda = 1.2$. The corresponding values of ϵ and f' can then be obtained from Fig. 2, and they are listed in Table II. Similar values for KBr are also listed there. According to Table II, agreement with experiment is good for KI, but for KBr, the theoretical ϵ is too high. It is not clear at this point to what extent the disagreement is due to uncertainties in W_1 and W_3, or to the mea-

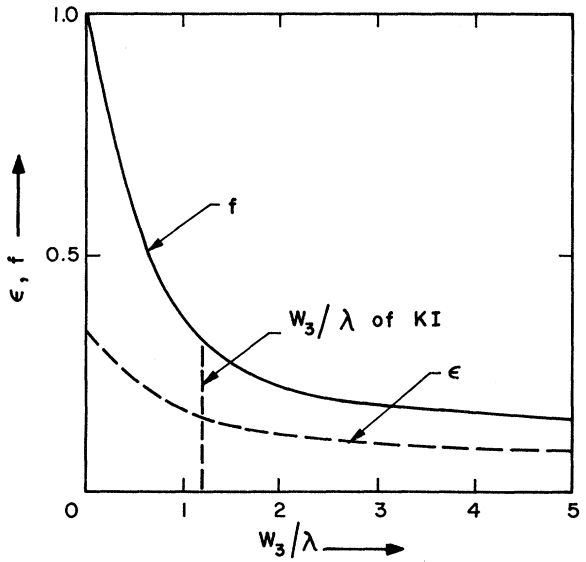

FIG. 2. f and ϵ as calculated by the method of Sec. V. The values shown are appropriate to a peak of the dichroism curve; they are plotted as a function of W_3/λ, where W_3 is the effective rms value of the noncubic-phonon vibrations, and where λ is the spin-orbit coupling parameter (see text).

TABLE III. Values of ϵ and f' for cesium halides, calculated according to Sec. V.

Crystal	W_1/λ	W_3/λ	f'_H	ϵ_H	f'_L	ϵ_L
CsCl	1.08	1.34	0.50	0.10	0.36	0.15
CsBr	2.0	1.85	0.40	0.11	0.29	0.15

sured value of ϵ, or to a breakdown in the adiabatic approximation. The explanation may well lie with the last of these, as mentioned earlier.

In this paper we are primarily concerned with the potassium halides. However, it was easy to repeat the calculations with input parameters suitable to the cesium halides as well. Therefore, for the sake of completeness, we list in Table III values of f' and ϵ computed for the F center in CsCl and CsBr. Since there is considerable asymetry in the results, separate values must be listed for the low-energy (L) and high-energy (H) dichroism peaks. In view of the large values of f', ϵ is surprisingly small for the cesium halides. The calculated values of f' agree rather well with the experimental data of Figs. 14 and 15 of Ref. 6. Unfortunately, ϵ has never been measured for the cesium halides.

Finally, we demonstrate the various band shapes that may be obtained from this model, calculated for the case of KI. Figure 3(a) shows a comparison between the observed MCD curve $[f'(E)]$ and the calculated one. The calculated curve is rather sensitive to W_1 and W_3; thus a good fit could be made by slight adjustment of these two away from the values taken from experiment. However, such a fit was not undertaken because of the large computer time required, and becuase such a precise fitting was not our major interest here. Instead, the values for W_1 and W_3 of Table VI in Ref. 6 were used. The calculated curve reproduces rather well the general features of the experimental MCD curve. In particular, it shows the same asymmetry as the measured one, the positive peak being somewhat more pronounced than the negative (long-wavelength) peak.

Figure 3(b) shows the computed absorption curve, and most importantly, it shows the computed values of $\epsilon(E)$. As mentioned earlier, ϵ is fairly constant over a wide range of the band. However, a sharp decrease of ϵ takes place in the far wings. The predicted behavior can be understood in terms of the different roles played by the cubic vs the noncubic modes. That is, in the middle of the band, the energy excursions are provided mainly by the cubic modes, and the nearly constant value of ϵ is obtained by averaging over all allowed values of the noncubic modes. But in the wings, the averaging process can extend only over large values of the noncubic coordinates, since large energy shifts of the absorbing state are mainly achieved by the combined extreme action of all the modes, Thus, in the far wings, we obtain the small ϵ that is associated with large noncubic distortions.

VI. CONCLUSIONS

The MCD effect and the spin memory in the optical-pumping cycle of F centers in alkali halides can be understood qualitatively by calculating the wave functions for various static distortions of the lattice that have nonzero matrix elements with the p-like absorption state. The important parameter is the strength of the interaction with the lattice distortion relative to the spin-orbit coupling parameter λ. By taking into account the dynamic character of the distortions in the frame of the adiabatic approximation, we obtain results in reasonably good agreement with experimental values; this is especially true for the heavier halides, where the conditions for the adiabatic condition are more nearly satisfied. Qualitatively, the calculations indicate that an MCD effect of moderate

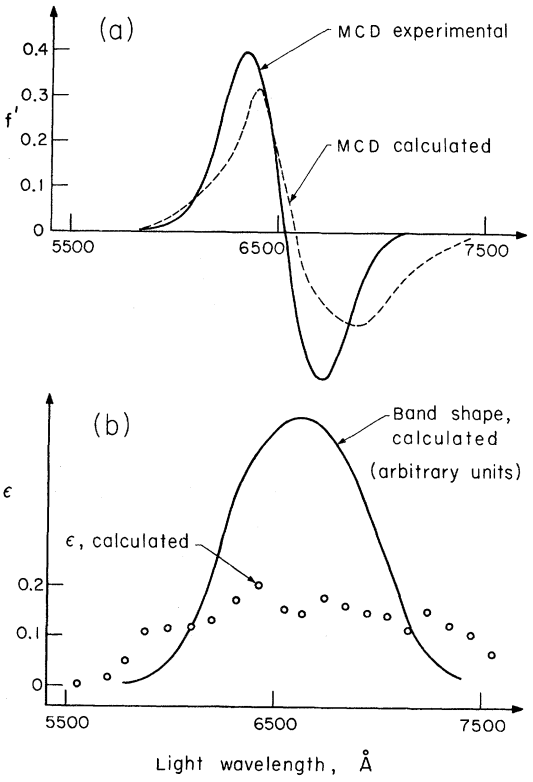

FIG. 3. (a) Experimental and calculated curves of the MCD fraction f' as a function of the light wavelength, for the F center in KI. Here f' has been normalized to the gross absorption at either of the peaks of the f' curve itself. (b) Calculated shape of the gross absorption, and calculated values of ϵ, as a function of light wavelength, for the F center in KI.

size is accompanied by a relatively small loss in spin memory. However, details depend on the relative strength of the cubic and noncubic modes. The usefulness of the model could be further checked by measuring the spin memory in the optical-pumping cycle of the F band of the cesium halides, and by investigating the change of ϵ with the photon energy.

*Research supported in part by the U. S. Atomic Energy Commission, Report No. UCB-34P20-150.

†Present address: Erstes Physikalisches Institut, Heidelberg, Germany.

[1]L. F. Mollenauer and S. Pan, preceding paper, Phys. Rev. B 6, 772 (1972).

[2]N. V. Karlov, J. Margerie, and Y. Merle-D'Aubigne, J. Phys. Radium 24, 717 (1963).

[3]J. Mort, F. Lüty, and F. C. Brown, Phys. Rev. 137, A566 (1965).

[4]L. F. Mollenauer, S. Pan, and S. Yngvesson, Phys. Rev. Letters 23, 683 (1969).

[5]C. H. Henry, S. Schnatterly, and C. P. Slichter, Phys. Rev. 137, A583 (1965).

[6]C. H. Henry and C. P. Slichter, in *Physics of Centers*, edited by W. B. Fowler (Academic, New York, 1968), p. 351.

[7]P. R. Moran, Phys. Rev. 137, A1016 (1965).

[8]M. Lax, J. Chem. Phys. 20, 1752 (1952).

[9]F. C. Brown, B. C. Cavenett, and W. Hayes, Proc. Roy. Soc. (London) A300, 78 (1967).

PHYSICAL REVIEW B VOLUME 6, NUMBER 3 1 AUGUST 1972

Spectroscopy of Cr^{3+} in $CsCr(SO_4)_2 \cdot 12H_2O/D_2O$, a β-Alum

Ludwig Grabner and Richard A. Forman
National Bureau of Standards, Washington, D. C. 20234

and

Eugene Y. Wong
Physics Department, University of California, Los Angeles, California 90024

(Received 20 December 1971)

The trigonal-field splitting of ^2E into $\bar{E}$ and $2\bar{A}$ states is found to be $\bar{E} - 2\bar{A} = -120$ cm^{-1} by identifying $2\bar{A}$. The no-phonon lines of deuterated samples are isotope shifted 6 cm^{-1} to the red. The following generalizations suffice to relate the spectra of the Cr-alums: (i) They are due to $^4A_2 \rightarrow \bar{E}$, $2\bar{A}(^2E)$ transitions. The splitting of ^2E is large for the β-alums, small for the α-alums. (ii) Sulfate-group disorder, found in all α-alums, complicates their spectra by adding inequivalent Cr^{3+} sites.

Sugano and Tanabe[1] have repeatedly called attention to the "difficulties in the problem of the Cr-alums." This is ironic because modern crystal-field theory, otherwise successful, originated in the work of Finkelstein and Van Vleck[2] which "laid down the method of calculation employed by all inquiry that followed."[3] We present new data on Cr^{3+} in pure $CsCr(SO_4)_2 \cdot 12H_2O/D_2O$, a β-alum. We conclude with the main point, a speculation on the relationship between structure and spectroscopy in all Cr-alums which proposes a resolution of the apparent "difficulties" using conventional crystal-field theory.

The formula of the alums is $A^+B^{3+}(RO_4)_2 \cdot 12H_2O$. A^+ is a monovalent cation (K, Rb, ...); B^{3+} is a trivalent metal ion (Al, Fe, ...); and R is S, Se, or Te. The unit cell contains four formula units. The space group is cubic $Pa3(T_h^6)$. Lipson[4] showed that the alums exhibit three types of structure which he named α, β, and γ. The structure is shown in Fig. 1. The caption summarizes the difference between the α, β, and γ structures. These have been refined by Cromer *et al.*[6] who find, in addition, that all α-alums show sulfate-group disorder consisting of some sulfate groups in reversed orientation along the threefold axis. Hausühl[7] classifies 65 alums: 40 (α), 24 (β), 1 (γ). The only known γ alum is $NaAl(SO_4)_2 \cdot 12H_2O$.

There are four equivalent Cr^{3+} in the unit cell: one on each of the four body diagonals. The nearest neighbors of Cr^{3+}, $6H_2O$'s, are arranged about the Cr^{3+} in a perfect octahedron.[4,6] The crystal field due to them is therefore cubic. However, the "distant" atoms, i.e., those other than nearest neighbors are arranged about Cr^{3+} in trigonal symmetry (C_{3i}).[8] These are bonded to the oxygens of the Cr^{3+} waters by hydrogen bonds[6] as shown in Fig. 1.

In spite of the fact that the Cr^{3+}-$6H_2O$ octahedron is undistorted, next-nearest neighbors may deform